Off-line and real-time monitoring of acetaminophen photodegradation by an electrochemical sensor

Silvia Berto, Luca Carena, Enrico Chiavazza, Matteo Marletti, Andrea Fin, Agnese Giacomino, Mery Malandrino, Claudia Barolo, Enrico Prenesti, Davide Vione. Off-line and real-time monitoring of acetaminophen photodegradation by an electrochemical sensor. Chemosphere 204 (2018) 556-562, doi: 10.1016/j.chemosphere.2018.03.069.

Off-line and real-time monitoring of acetaminophen photodegradation by an electrochemical sensor

Silvia Berto[1], Luca Carena[1*], Enrico Chiavazza[1], Matteo Marletti[1], Andrea Fin[2], Agnese Giacomino[3], Mery Malandrino[1], Claudia Barolo[1,4], Enrico Prenesti[1], Davide Vione[1]

[1] *Dept. of Chemistry, University of Torino, Via P. Giuria 7, 10125 Turin, Italy*

[2] *Dept. of Chemistry and Biochemistry, University of California, San Diego, La Jolla, California 92093-0358, United States*

[3] *Dept. of Drug Science and Technology, University of Torino, Via P. Giuria 9, 10125 Turin, Italy*

[4] *INSTM and NIS Centre, University of Torino, Via Quarello 15A, 10135 Turin, Italy*

*Corresponding author:
E-mail address: luca.carena@unito.it; silvia.berto@unito.it.
Telephone: 0039 0116705296
Postal address: Via P. Giuria, 5, 10125 Torino, Italy

Abstract

The photochemistry of N-acetyl-para-aminophenol (acetaminophen, APAP) is here investigated by using differential pulse voltammetry (DPV) analysis to monitor APAP photodegradation upon steady-state irradiation. The purpose of this work is to assess the applicability of DPV to monitor the photochemical behaviour of xenobiotics, along with the development of an electrochemical set-up for the real-time monitoring of APAP photodegradation. We here investigated the APAP photoreactivity towards the main photogenerated reactive transients species occurring in sunlit surface waters (hydroxyl radical $HO^{\bullet}$, carbonate radical $CO_3^{\bullet-}$, excited triplet state of anthraquinone-2-sulfonate used as proxy of the chromophoric DOM, and singlet oxygen $^1O_2$), and determined relevant kinetic parameters. A standard procedure based on UV detection coupled with

liquid chromatography (HPLC-UV) was used under identical experimental conditions to compare and verify the DPV-based results. The latter were in agreement with HPLC data, with the exception of the triplet-sensitized processes. In the other cases, DPV could be used as an alternative to the well-tested but more costly and time-consuming HPLC-UV technique. We have also assessed the reaction rate constant between APAP and $HO^{\bullet}$ by real-time DPV, which allowed for the monitoring of APAP photodegradation inside the irradiation chamber. Unfortunately, real-time DPV measurements are likely to be affected by temperature variations of the irradiated samples. Overall, DPV appeared as a fast, cheap and reasonably reliable technique when used for the off-line monitoring of APAP photodegradation. When a suitable real-time procedure is developed, it could become a very straightforward method to study the photochemical behaviour of electroactive xenobiotics.

Keywords

Acetaminophen; Paracetamol; Glassy carbon electrode; Photochemistry; Electrochemistry; Differential Pulse Voltammetry

1. Introduction

For several years to date some classes of xenobiotic compounds, defined as "Contaminants of Emerging Concern – CECs" by the US-EPA (Environmental Protection Agency), have been detected at low but significant levels in wastewaters and in surface waters (Zuccato et al., 2005; OW/ORD Emerging Contaminants Workgroup, 2008). Pharmaceuticals and personal care products (PPCPs) along with nanoparticles are CECs that often occur in the wastewater treatment plants (WWTPs) influents, as well as in water bodies such as lakes, rivers and coastal waters (Heberer, 2002; Zuccato, 2004; Zuccato et al., 2006; Pojana et al., 2009). These compounds are usually water-soluble and not completely biodegradable, and they often survive the WWTPs treatments such as those based on activated sludge. WWTPs were not originally designed to eliminate xenobiotics, thus their removal efficiencies range in a wide interval (Ternes, 1998; Stumpf et al., 1999).

The presence of CECs in surface waters is alarming, both because of the potential ecosystems damage and for the possible generation of transformation intermediates and products (TPs) of high environmental concern. In this context, the photochemical reactions taking place in sunlit surface waters play an important role in the attenuation of xenobiotics and/or the generation of problematic TPs. Photochemical reactions are generally divided into direct photolysis and indirect photochemistry. Direct photolysis occurs when a compound (e.g., a xenobiotic) absorbs sunlight to reach molecular excited states or lose an electron, thereby undergoing chemical transformation. In contrast, an indirect phototransformation occurs when the xenobiotic reacts with photochemically produced reactive intermediates (PPRIs) such as hydroxyl radicals ($HO^{\bullet}$), carbonate radicals ($CO_3^{\bullet-}$), excited triplet states of chromophoric dissolved organic matter (^{3}CDOM*) and singlet oxygen ($^1O_2$). PPRIs are formed upon absorption of sunlight by naturally occurring photosensitizers such as most notably CDOM, nitrate and nitrite (Vione et al., 2014). Photochemical reactions usually act as self-depuration processes in water bodies, but they can also induce the formation of harmful TPs (Vogna et al., 2004; Erickson et al., 2012).

The photochemical fate (half-life times and intermediates photoproduction) of xenobiotics in sunlit surface waters can be predicted by suitable photochemical models, once the key photoreactivity parameters are known (Minella et al., 2016; Carena et al., 2017). Among these parameters, the direct photolysis quantum yields and the second-order rate constants for the reactions between PPRIs and xenobiotics play a key role. The rate constants can be measured by time-resolved techniques such as the laser flash photolysis (LFP), or by steady-state irradiation experiments. The LFP measurements require expensive instrumentation and, in some cases, they do not provide the actual reaction rate constants (Canonica et al., 2006), for instance because of physical quenching phenomena. In contrast, the steady-state irradiation experiments are more accessible and may provide reliable results despite longer experimental protocols.

Steady-state experiments usually require: (i) the steady-state irradiation of solutions containing the studied xenobiotic and a photosentizer, which generates selectively a PPRI upon light absorption; (ii) the sampling of the irradiated solution after different irradiation times, and (iii) sample analysis by using suitable analytical techniques, such as very often the High Performance Liquid Chromatography interfaced with a UV/Vis detector (HPLC-UV). In the case of N-acetyl-para-aminophenol (APAP), a widely used analgesic and antipyretic drug known as acetaminophen or paracetamol, the detailed HPLC-UV protocol for the determination of its main photoreactivity parameters is reported elsewhere (De Laurentiis et al., 2014).

Although HPLC-UV is often used in photodegradation studies of organic pollutants, electrochemistry could be an alternative. Previous works have described the use of electrochemical techniques to monitor the photodegradation of pharmaceuticals (Hu et al., 2010; Wei et al., 2012) and pesticides (Rahemi et al., 2015), by using an experimental approach that consists in the irradiation, sampling and analysis of solutions.

In the present work, we introduce an electrochemical set-up to study the photochemistry of APAP, a CEC that is frequently detected in WWTPs and surface waters (Peuravuori, 2012; Stamatis and Konstantinou, 2013). In the new proposed set-up we used the differential pulse voltammetry (DPV)

and an electrochemically activated glassy carbon electrode (GCE), which has been previously developed for the quantification of APAP in aqueous solutions (Chiavazza et al., 2016). To assess the reliability of the DPV protocol, we compared the relevant results with those obtained by using the HPLC-UV technique. Initially, the photochemical experiments were carried out with the standard off-line procedure (irradiation, sampling, analysis), both by using DPV and HPLC-UV detection. Finally, the DPV set-up was implemented into a real-time monitoring system of APAP photodegradation, unifying the three steps of the off-line procedure in an overall simpler, time-saving and more straightforward approach.

2. Materials and methods

2.1. Reagents

Acetaminophen (APAP, purity grade >99%), anthraquinone-2-sulfonic acid, sodium salt (AQ2S, 97%), KNO_3 (>99%), $NaHCO_3$ (98%), H_3PO_4 (85%), $NaH_2PO_4 \cdot H_2O$ (98%), KH_2PO_4 (≥99%), $Na_2HPO_4 \cdot 2H_2O$ (98%), $Na_2B_4O_7$ (>99%), NaOH (99%) and 2-nitrobenzaldehyde (98%) were purchased from Sigma Aldrich, 2-propanol (for residue analysis) from Merck, methanol (gradient grade) from Carlo Erba, Rose Bengal (RB) from Alfa Aesar, $NaNO_3$ (99.5%) from BDH. Ultrapure water from a Millipore system was used to prepare all the solutions (resistivity >18 MΩ cm, organic carbon < 2 μg_C L^{-1}). The borate-phosphate buffer (BPB) solution used for the electrochemical activation of GCE was prepared by dissolving KH_2PO_4 (or Na_2HPO_4) and $Na_2B_4O_7$ salts to a final concentration of 4.5×10^{-2} and 0.5×10^{-2} mol L^{-1}, respectively, and by adjusting the pH to 9.0 ± 0.1 with 1 mol L^{-1} NaOH (or 85% H_3PO_4). The phosphate buffer (PB, 5×10^{-2} mol L^{-1}) solution used for the electrochemical analysis and the (real-time) irradiation experiments was prepared by dissolving KH_2PO_4 and by adjusting the pH to 7.0 ± 0.1 with 1 mol L^{-1} NaOH. The pH was

measured with an Amel mod. 338 pH-meter (resolution of ±0.1 mV), equipped with a Metrohm combined glass-electrode (mod. 6.0234.100).

2.2. Irradiation experiments

APAP solutions were placed into a square Pyrex glass bottle (capacity 100 mL) and irradiated for up to 3 or 6 h with a Philips PL-S 9W/01/2P lamp (emission maximum at 313 nm). The bottle was placed vertically and the lamp radiation was incident on one of the bottle flat sides. The lamp spectrum is reported in the Supplementary Material (hereafter SM, Figure SM1) and it was assessed actinometrically by using 2-nitrobenzaldehyde as chemical actinometer (Galbavy et al., 2010). The detailed protocol for the 2-nitrobenzaldehyde actinometry is reported elsewhere (Marchisio et al., 2015). Differently from Marchisio et al. (2015), 5.0×10^{-4} mol L^{-1} 2-nitrobenzaldehyde solutions (with volumes of 50 and 100 mL to match the different irradiation experiments) were irradiated under the UVB lamp. The APAP concentration and the volume of the irradiated solutions were chosen to enable the subsequent chromatographic and voltammetric measurements or the immersion of the electrochemical probes in the solution contained inside the bottle. The solutions were continuously stirred during irradiation. Depending on the reactive transient species or the process to be studied, the following conditions were used:

Direct Photolysis. Irradiation of 1.0×10^{-5} mol L^{-1} APAP and 5.0×10^{-3} mol L^{-1} PB at pH 7.0.

Hydroxyl Radicals ($HO^{\bullet}$). Competition kinetics experiments between APAP and 2-propanol. The APAP initial concentration was $2.0\cdot10^{-5}$ mol L^{-1} (unless otherwise reported), while the alcohol concentration varied from 0 to 1.0×10^{-3} mol L^{-1}, with intermediate concentration values of 25, 50, 100, 300 and 500 μmol L^{-1}. These experiments were carried out to assess the rate constant of the APAP+$HO^{\bullet}$ reaction. Nitrate (5.0×10^{-3} mol L^{-1} $NaNO_3$) under irradiation was used as photochemical $HO^{\bullet}$ source (Mack and Bolton, 1999).

Carbonate Radicals ($CO_3^{\bullet-}$). Irradiation of 2.0×10^{-5} mol L^{-1} APAP and 5.0×10^{-3} mol L^{-1} KNO_3, with addition in different experiments of $NaHCO_3$ at concentrations of 5.0×10^{-3} and 1.0×10^{-2} mol L^{-1} (pH 7.70 and 7.95, respectively), or of NaH_2PO_4 at 5.0×10^{-3} and 1.0×10^{-2} mol L^{-1} (pH 7.70 and 7.95, respectively).

Excited Triplet States ($^3AQ2S^*$). Anthraquinone-2-sulfonate (AQ2S) was used as CDOM proxy molecule, due to the widespread occurrence of quinonoid moieties in CDOM (Cory and McKnight, 2005), and because the irradiation of AQ2S selectively produces the triplet state without forming other reactive intermediates, such as $^1O_2$ and $HO^{\bullet}$. The photochemical behaviour of AQ2S is well known (Loeff et al., 1983; Bedini et al. 2012) and this compound is experimentally very convenient. However, it may be more photoactive than average CDOM (Avetta et al., 2016) because its triplet state is a stronger oxidant than the natural $^3CDOM^*$ (McNeill and Canonica, 2016). The irradiated solutions contained APAP at concentration levels of 5.0×10^{-6}, 1.0×10^{-5} and 2.0×10^{-5} mol L^{-1} in different experiments, as well as 1.0×10^{-4} mol L^{-1} AQ2S and 5.0×10^{-3} mol L^{-1} PB at pH 7.0.

Singlet Oxygen ($^1O_2$). Rose Bengal (RB) was used as photochemical source of $^1O_2$. The irradiated solutions contained 2.0×10^{-5} mol L^{-1} APAP, 1.0×10^{-5}, 2.5×10^{-5} and 5.0×10^{-5} mol L^{-1} RB in different experiments, and 5.0×10^{-3} mol L^{-1} PB (pH 7.0).

The time trend of APAP was monitored by two alternative procedures, namely an off-line one with both DPV and HPLC-UV detection, and (only for APAP + $HO^{\bullet}$) a real-time method where the DPV set-up was immersed into the irradiated solution.

2.2.1. Off-line procedure

Solutions (50 mL) containing APAP and the relevant photosensitizers ($NaNO_3$, KNO_3 + $NaHCO_3$, AQ2S, RB) were irradiated for 3 h, while the direct photolysis of APAP was assessed by irradiating the solutions for 6 h. At scheduled irradiation times, sample aliquots of 1 and ~1.5 mL were taken

from the irradiated solutions and analyzed by DPV and HPLC-UV, respectively. The aliquots for HPLC-UV analysis were injected directly, and the chosen volume ensured that the vials were filled enough for autosampler injections. The aliquots for the DPV analysis were further diluted ten times with PB 5.0×10^{-2} mol L^{-1} to enable a reasonable capacitive current. PB generally did not occur in the irradiated solutions, but some irradiation runs were carried out in the presence of PB at low concentration to minimize pH changes.

2.2.2. Real-time procedure

The real-time procedure was tested in the case of the APAP + $HO^{\bullet}$ reaction alone. Each irradiated solution (100 mL, to ensure proper immersion of the DPV set-up) initially contained 5.0×10^{-3} mol L^{-1} $NaNO_3$ and 5.0×10^{-2} mol L^{-1} PB as supporting electrolyte at pH 7.0. The DPV set-up was immersed into the solution that was then irradiated for 1 h with the previously described UV lamp. This pre-irradiation step allowed for the solution to reach temperature values (40-45°C) where the APAP DPV-signals undergo limited variation with temperature. After this pre-irradiation period, the steady-state irradiation experiment was started by addition of small volumes of APAP (~1 mL) and 2-propanol (max. volume ~1 mL) to reach concentrations values of 2.15×10^{-5} mol L^{-1} (APAP) and variable from 0 to 1×10^{-3} mol L^{-1} (2-propanol). The APAP quantification was carried out by DPV every ~3 min, starting from the beginning of the irradiation.

2.3. Electrochemical measurements

The electrochemical measurements and treatments (both off-line and real-time) were performed with a Bio-Logic SP150 potentiostat, using a conventional three-electrode system. Electrochemically activated GCE (3×10^{-3} m diameter, purchased from ALS Co., Ltd) was used as working electrode, a platinum wire as counter electrode, and Ag/AgCl, 3 mol L^{-1} KCl (Metrohm,

Model 6.0733.100) as reference electrode. A magnetic stirrer switched on upon irradiation ensured the convective transport during the amperometric measurements. The electrochemical procedures for the quantification of APAP have already been optimized in previous work (Chiavazza et al., 2016) and are summarized below.

Activation step. The working electrode was mechanically polished with diamond powder (d=1 μm) and alumina (d=0.3 μm), both by ALS Co., Ltd. The electrode was then immersed in acetonitrile for 1 min and thoroughly washed with ultra-pure water. The electrochemical activation was carried out in BPB solution by applying an anodic potential of +2.0 V for 60 s under magnetic stirring, and it was followed by chronoamperometry. The activated electrode was then directly used for the measurements inside the PB-containing solutions.

Measurements. In the off-line procedure the measurements were carried out at room temperature, while for the real-time experiments the temperature was higher because of the lamp heating the solutions. As reported above, solutions were pre-irradiated for 1 h to reach stable measurements conditions. In both the off-line and real-time cases the measurement included a brief conditioning period (5 s) of the GCE at +2.0 V under magnetic stirring. The DPV parameters were as follows: step height 5×10^{-3} V, pulse amplitude 5×10^{-2} V, pulse length 5×10^{-2} s, pulse period 0.100 s and potential range between 0.05 and 0.70 V. Overall, the peak current of the APAP signal was recorded at ~335 mV. Before APAP quantification, some DPV measures on blank solutions (about 5 replicates) were performed in order to reach a stable and reliable signal. Note that, for the real-time procedure, the blank solution was that undergoing the pre-irradiation step. During that procedure the solution was continuously stirred and irradiated but, 1 min before and during the DPV measures, stirring and irradiation were stopped. The procedure was made easier by the fact that the potentiostat allowed for the control of the stirrer and of the lamp during each analytical sequence.

2.4. Chromatographic determinations

The irradiated solutions were analyzed by HPLC-UV, using a VWR-Hitachi LaChrom Elite chromatograph equipped with L-2200 autosampler (injection volume 60 μL), L-2130 quaternary pump for low-pressure gradients, Duratec vacuum degasser, L-2300 column oven (set at 40 °C), and L-2455 photodiode array detector. The column was a VWR LiChroCART 125-4 Cartridge, packed with LiChrospher 100 RP-18 (125mm×4mm×5μm). Elutions were carried out in isocratic mode with a mixture of 90% A (aqueous H_3PO_4 at pH ~2.8) and 10% B (methanol), with a total flow rate of 1.0 mL min^{-1} (column dead time 1.4 min). The elution time of APAP, detected at 244 nm, was 6.2 min.

2.5. Kinetic data treatment

In the off-line experiments, the time trends of APAP under irradiation followed pseudo-first order kinetics (Figure SM2). Therefore, the reaction rates were determined by fitting the time evolution data with the equation $S_t\ S_o^{-1} = e^{-kt}$, where S_t is the APAP instrumental signal (obtained by either DPV or HPLC-UV) at the irradiation time t, S_o is the signal corresponding to the APAP initial concentration (C_o), and k is the pseudo-first order degradation rate constant. The numerical fit of the experimental data yielded the value of k for each relevant irradiation run. The linearity and the negligible intercept of the APAP calibration curves from 2.5×10^{-7} to 2.5×10^{-6} mol L^{-1} (DPV measurements) and from 1.0×10^{-6} to 3.5×10^{-5} mol L^{-1} (HPLC-UV measurements) concentration allowed for the use of the relationship $S_t\ S_o^{-1} = C_t\ C_o^{-1}$, where C_t is the APAP concentration at the irradiation time t. Therefore, the initial degradation rates were calculated as $R_{APAP}^{tot} = k\ C_o$. Note that R_{APAP}^{tot} includes the rates of all the possible reactions that induce the degradation of APAP under irradiation. In the real-time experiments, the APAP time trend was fitted with the equation (exponential function with a residual) $C_t\ C_o^{-1} = 1 - A\ (1 - e^{-kt})$, where A and k were obtained by

numerical fit (Figure SM2). APAP was quantified by calibration curves with the form $S_t = m \cdot C_t + q$, where m is the slope and q the non-zero intercept, obtained by varying C_t in the linear range from 9.8×10^{-6} to 2.3×10^{-5} mol L^{-1} in solutions that underwent 1h of pre-irradiation time. The initial reaction rates were then computed as $R_{APAP}^{tot} = A\,k\,C_o$. The error bounds to the rates represent the goodness of the fit of the time-trend data, combined with error propagation from k and A to R_{APAP}^{tot}. Some experimental replicas were carried out, with a reproducibility of ~10-20% (relative standard deviation of R_{APAP}^{tot}).

3. Results and Discussion

3.1. Off-line study of APAP photochemistry

Direct Photolysis. Upon 6 h of irradiation, APAP degradation was quantified as ~14% of the initial substrate and the trends obtained by DPV and HPLC-UV were in good agreement (Figure 1).

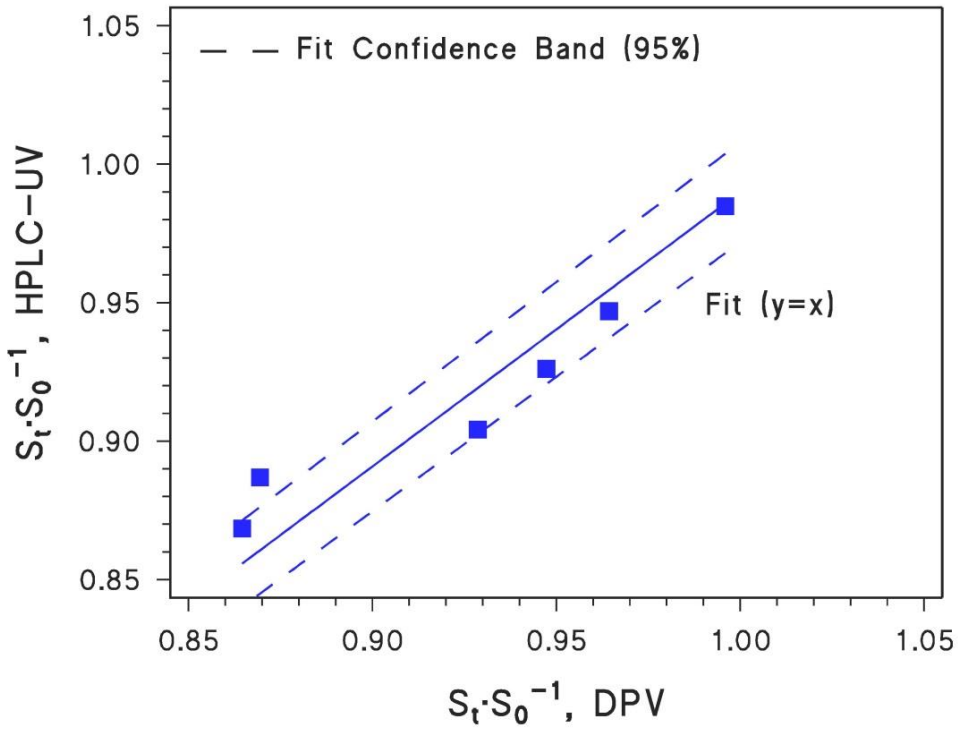

Figure 1. Correlation plot showing the good agreement between DPV and HPLC-UV measurements in the direct photolysis experiments (off-line procedure). The R^2 parameter of the fit was ~0.9277 (minR^2 ~ 0.6583, with α = 5%).

Reaction with Hydroxyl Radicals (HO•). The degradation rates of APAP in competition experiments with 2-propanol are reported in Figure 2. Scheme 1 shows the possible reactions taking place into the irradiated solutions (De Laurentiis et al., 2014).

The DPV and HPLC-UV results were in reasonable agreement as depicted in Figure 2, although the values obtained with DPV were a bit higher. Eq. 1 describes the initial degradation rate of APAP (R_{APAP}^{tot}) as a function of the concentration of 2-propanol ([2-Pr]), and it was obtained from Scheme 1 by applying the steady-state approximation to both HO• and R•:

$$R_{APAP}^{tot} = R_{HO^\bullet}^{NO_3^-}\left(\frac{k_2[APAP]}{k_2[APAP]+k_1[2-\mathrm{Pr}]}+\frac{k_1[2-\mathrm{Pr}]}{k_2[APAP]+k_1[2-\mathrm{Pr}]}\times\frac{k_3[APAP]}{k_3[APAP]+\sum_i k_i[S_i]}\right) \quad (1)$$

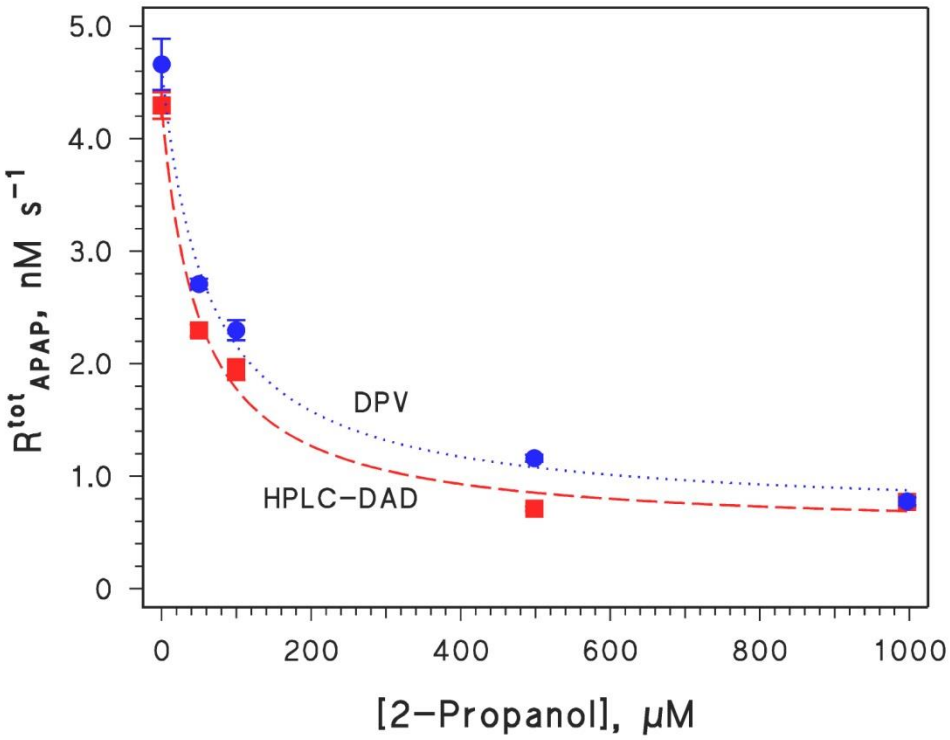

Figure 2. Off-line experiments: degradation rates of APAP under irradiation at different 2-propanol concentrations values. The DPV and the HPLC-UV data were fitted with Eq. 1, which provided the second-order reaction rate constant between APAP and $HO^{\bullet}$ (k_2).

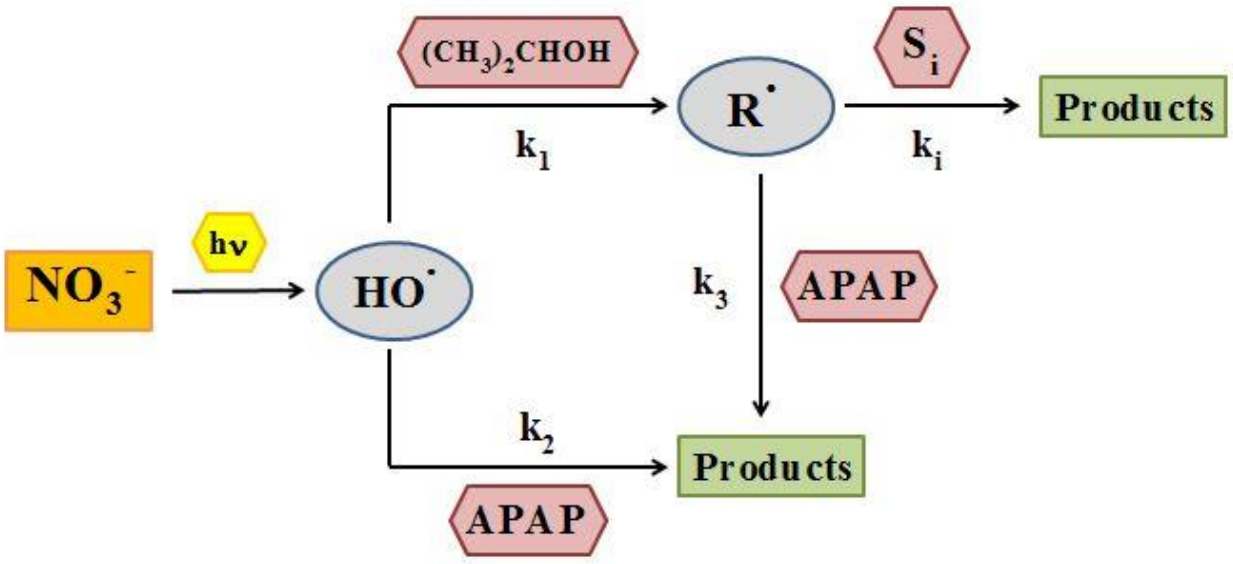

Scheme 1. Main reactions taking place in the irradiated solutions, as the basis to obtain Eq.1. Note that $(CH_3)_2CHOH$ = 2-propanol and R· means 'radical species'. They may be organic radicals derived from 2-propanol or $HO_2^{\bullet}/O_2^{\bullet-}$, produced by reaction between some organic radicals and dissolved O_2.

In Eq. (1), $R_{HO^\bullet}^{NO_3^-}$ is the formation rate of HO$^\bullet$ by nitrate photolysis, k_1 = 1.9·10^9 L mol^{-1} s^{-1} is the second-order rate constant for the reaction between 2-propanol and HO$^\bullet$ (Buxton et al., 1988), k_2 = $k_{APAP+HO^\bullet}$ is the second-order reaction rate constant between APAP and HO$^\bullet$, k_3 the second-order reaction rate constant between APAP and R$^\bullet$ (where the radicals R$^\bullet$ are formed from 2-propanol and HO$^\bullet$), and $\sum_i k_i[S_i]$ (overall a first-order rate constant, obtained as the sum of several second-order processes) describes the scavenging of R$^\bullet$ by a series of compounds that occur in the irradiated solution (e.g., the APAP photoproducts). The direct photolysis was not taken into account because, in the time range of the nitrate experiments (3 h), APAP did not undergo a significant photodegradation when irradiated alone.

The fit of the experimental data with Eq. 1 was best achieved by using $R_{HO^\bullet}^{NO_3^-}$, k_2 and $\alpha = k_3[APAP]\ (k_3[APAP] + \sum_i k_i[S_i])^{-1}$ as fit variables. The main target was the determination of k_2 = $k_{APAP+HO^\bullet}$, which was quantified as (5.82±1.10)×10^9 L mol^{-1} s^{-1} and (4.82±1.09)×10^9 L mol^{-1} s^{-1} by using the data obtained with DPV and HPLC-UV, respectively (the error bounds represent the fit standard deviations). The two values are not significantly different, thereby suggesting that the two techniques provide comparable results. Furthermore, our k_2 values are very similar to those obtained in previous studies by Szabó et al. (2012) with pulse radiolysis (5.6×10^9 L mol^{-1} s^{-1}) and by El Najjar et al. (2014) (4.9×10^9 L mol^{-1} s^{-1}, steady irradiation experiments). Different values for the same rate constant, although of the same order of magnitude, have been reported by Andreozzi et al. (2003) (2.2×10^9 L mol^{-1} s^{-1}), Yang et al. (2009) (1.7×10^9 L mol^{-1} s^{-1}) and De Laurentiis et al. (2014) (1.8×10^9 L mol^{-1} s^{-1}) using steady-state irradiation, as well as by Bisby and Tabassum (1988) (9.7×10^9 L mol^{-1} s^{-1}) using pulse radiolysis.

Carbonate Radicals ($CO_3^{\bullet-}$). The reactivity of $CO_3^{\bullet-}$ with APAP was evaluated by a semi-quantitative screening method based on the irradiation of APAP solutions containing nitrate and bicarbonate, or nitrate and a phosphate buffer at the same concentration and pH as bicarbonate (Avetta et al., 2016). The aim of these experiments is to evaluate whether the substrate shows high reactivity toward $CO_3^{\bullet-}$, or whether the $CO_3^{\bullet-}$ reactivity is negligible compared to $HO^{\bullet}$. To do so one has to disentangle the photochemical and the pH effects of the addition of bicarbonate, which accounts for the use of the PB for pH adjustment in additional experiments. The kinetic data (first-order degradation rate constants) reported in Table SM1 show that APAP degradation was accelerated by the increase in pH produced by PB addition, but than an even higher acceleration at the same pH values was caused by the addition of bicarbonate. Because nitrate yields $HO^{\bullet}$ that produces $CO_3^{\bullet-}$ upon oxidation of HCO_3^- and CO_3^{2-}, with carbonate occurring in lower concentration but reacting faster with $HO^{\bullet}$, this result suggests that the reaction between APAP and $CO_3^{\bullet-}$ could be important in surface waters (Avetta et al., 2016), in agreement with the findings of De Laurentiis et al. (2014), who found a second-order reaction rate constant of $3.8 \cdot 10^8$ L mol^{-1} s^{-1}. To check for the possible importance of the direct photolysis of APAP under the studied conditions, some runs were also carried out in the presence of bicarbonate but without nitrate. The results of these experiments (data not reported) showed a much slower kinetics of APAP direct photolysis (by one-two orders of magnitude) compared to the degradation of APAP by $HO^{\bullet}$ + $CO_3^{\bullet-}$. Most importantly, the results obtained by using DPV agreed very well with those obtained by HPLC-UV (Table SM1).

Excited Triplet States (^{3}AQ2S*). AQ2S was used as a proxy molecule for CDOM, to assess the reactivity of APAP with ^{3}CDOM*. When irradiated, AQ2S forms the excited triplet state ^{3}AQ2S* that undergoes several deactivation processes including the reactions with water (thermal deactivation or production of transformation intermediates), with the AQ2S ground state, or with

other molecules (Bedini et al., 2012). The occurrence of AQ2S transformation products was observed in the DPV measures in the form of voltammetric peaks, and it was confirmed by irradiating a solution containing 1.0×10^{-4} mol L^{-1} AQ2S and 5.0×10^{-3} mol L^{-1} PB (pH 7). Unfortunately, one or more AQ2S photoproducts partially interfered with the DPV signals of APAP which, as a consequence, were not entirely resolved (Figure SM3). For this reason, it was not possible to obtain a reliable assessment of the reactivity between APAP and $^{3}AQ2S^{*}$ by using the DPV technique. The photodegradation trends of APAP measured with DPV showed higher APAP concentration values compared to HPLC-UV, in particular at high irradiation times, when the AQ2S photoproduct(s) would be more concentrated and could most easily affect the DPV measures.

Singlet Oxygen ($^{1}O_2$). The reaction between APAP and $^{1}O_2$ was studied by using RB as photosensitizer. RB is a pink dye that forms an excited triplet state under irradiation ($^{3}RB^{*}$). $^{3}RB^{*}$ quickly deactivates by reacting with ground-state O_2 to form $^{1}O_2$. RB solutions at increasing concentration enhanced the APAP degradation rate, which would reflect the increase of $^{1}O_2$ formation with increasing RB. However, the APAP signals obtained by DPV were sometimes underestimated at high RB concentrations ($\sim5\times10^{-5}$ mol L^{-1}) compared to the HPLC-UV data, probably due to the adsorption of RB onto the GCE surface. That could be visually verified because the electrode turned pink. The DPV data were also affected by a high signal variability. However, steady-state irradiation experiments to assess the reactivity with $^{1}O_2$ are usually carried out at relatively low RB concentrations ($<5\times10^{-5}$ mol L^{-1}), where the adsorption of RB does not affect the DPV signals significantly and the results obtained by DPV and by HPLC-UV are comparable (see Figure SM4).

3.2 Real-time monitoring of APAP photodegradation

The measurement of the $HO^{\bullet}$ second-order reaction rate constant was also carried out by using the real-time protocol, which was not employed to assess APAP reactivity towards $^{3}AQ2S^{*}$ and $^{1}O_2$ because of the aforementioned problems.

A 1-hour pre-irradiation step of the solutions was required before APAP photodegradation experiments, because an irradiation-time-dependent enhancement of the DPV signals was observed in solutions that were pre-irradiated and then spiked with APAP to reach a concentration of 2.0×10^{-6} mol L^{-1}. The signal enhancement reached a plateau a bit before 1-hour pre-irradiation. The signal increase was not strictly connected with irradiation itself: a 15-24% increase of the APAP peak current after 1.5 h was observed in the presence of 5.0×10^{-3} mol L^{-1} $NaNO_3$ + 5.0×10^{-2} mol L^{-1} PB (pH 7.0), both when irradiated with and without 1.0×10^{-3} mol L^{-1} 2-propanol, as well as in the dark. The system in the dark was covered with a double aluminum foil and placed under the lamp, to prevent light exposure while maintaining comparable temperature and stirring conditions as the irradiated solutions. The reported findings suggest that the enhancement of the APAP signals could be largely accounted for by the increase in solution temperature, which is one of the consequences of irradiation. The highest enhancement (24%) was anyway observed for the irradiated solution containing $NaNO_3$ + PB, without 2-propanol. In this system, $HO^{\bullet}$ is expected to occur at the highest levels due to nitrate photolysis and the absence of the alcohol as scavenger. The radical $HO^{\bullet}$ could cause an 'indirect photoactivation' of the electrode by reacting with the GCE surface (Rapecki et al., 2010), and this effect would be added to that of the temperature.

Figure 3 shows the voltammetric profiles of APAP photodegradation recorded every ~ 3 min during a real-time measurement after the needed pre-irradiation time (note that the pre-irradiated solution did not contain either APAP or 2-propanol). The APAP peak decreased with increasing irradiation time, and a new peak appeared at ~485 mV and it increased with irradiation time. The latter signal started decaying at high irradiation times and it was not detected in the DPV-based off-line

procedure, probably because it was due to a short-living photo-product or because of the sample dilution by a factor of 10 before APAP off-line electrochemical quantification (see Section 2.2.1), a dilution step that was not carried out in the real-time measurements. Unfortunately, the DPV technique did not allow further pieces of information to be collected concerning the nature of such an intermediate.

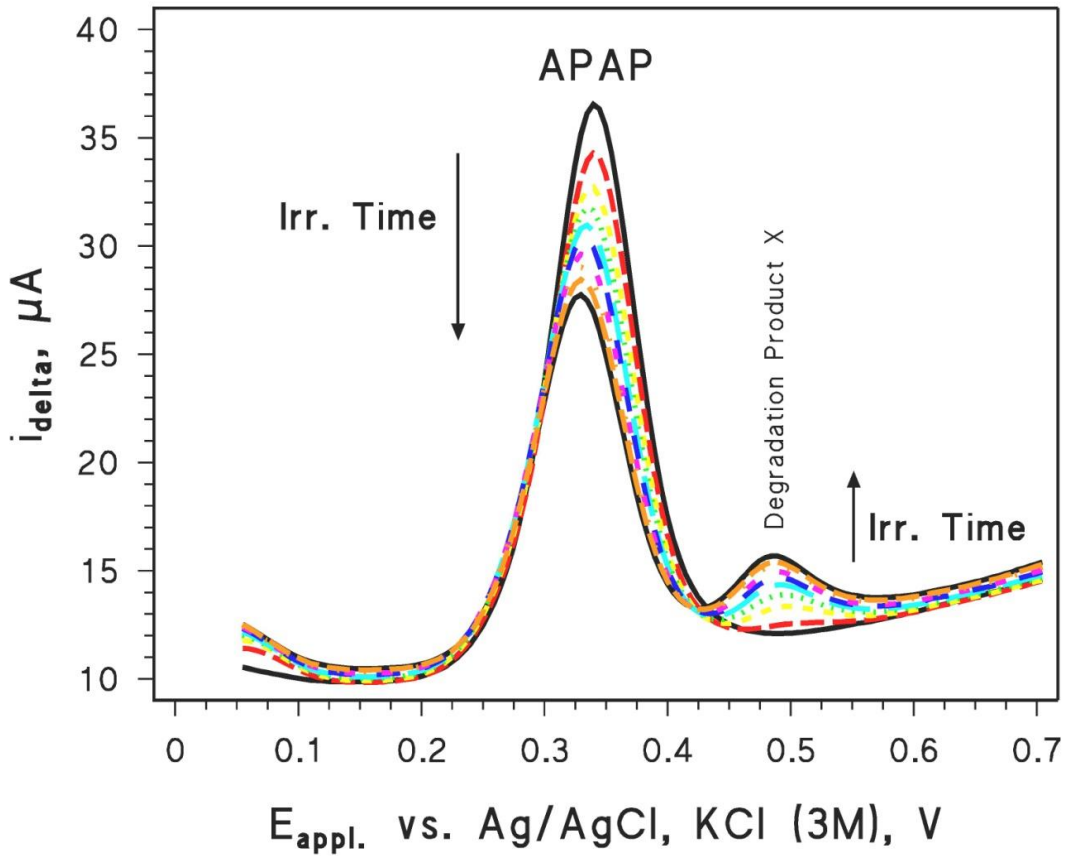

Figure 3. Real-time voltammetric profiles of APAP photodegradation recorded every 3 min. The concentration of 2-propanol was $5.0 \cdot 10^{-5}$ mol L^{-1}. Other chemical composition data are reported in the main text.

The $k_2 = k_{APAP+HO^{\bullet}}$ value obtained in the real-time experiments ($k_2 = (9.82 \pm 2.76) \times 10^9$ L mol^{-1} s^{-1}), despite a good fit of the experimental curve (Figure SM5) is quite far from those obtained with the off-line procedure ($(5.82 \pm 1.10) \times 10^9$ L mol^{-1} s^{-1} and $(4.82 \pm 1.09) \times 10^9$ L mol^{-1} s^{-1}), but it coincides

with that reported by Bisby and Tabassum (1988). We checked for the possible involvement of PB in this difference because in the real-time monitoring of APAP photodegradation, differently from the off-line protocol, the electrochemical sensor was immersed into the irradiated solution. Therefore, PB (5×10^{-2} mol L^{-1}, pH 7.0) had to be added as supporting electrolyte to the solution to allow DPV measurements. Note that, in the off-line protocol, the solution in some cases contained PB at lower concentration (5.0×10^{-3} to 1.0×10^{-2} mol L^{-1} as per the $CO_3^{\bullet-}$ reactivity measurements) to avoid pH variations during irradiation. PB can react with $HO^{\bullet}$ radicals (Buxton et al., 1988) and provide a further competition term in addition to the reactions of APAP + $HO^{\bullet}$ and 2-propanol + $HO^{\bullet}$. A kinetic scheme (see SM for further details) was developed to check for a possible effect of PB, but the result we obtained is that, although the PB role cannot be totally neglected, it cannot account for the observed difference in the $HO^{\bullet}$ second-order reaction rate constant between real-time and off-line experiments. Therefore, we speculate that temperature variations during the irradiation of the solutions may affect the real-time electrochemical measurements and thus the assessment of the APAP degradation rate, despite the efforts to limit these effects by pre-irradiating the solutions and by quantifying APAP with calibration curves obtained in the pre-irradiated solutions (see sections 2.2.2 and 2.5 for further details).

4. Conclusions

The study of the photochemical behaviour of emerging contaminants is of great environmental importance because of their widespread occurrence in sunlit surface waters and the potential effects of photochemical reactions on their transformation, with either depollution or production of harmful by-products.

In this work, we used DPV with an electrochemically activated GCE to study APAP photochemistry in steady-state irradiation experiments. The DPV results were compared with those obtained by

using the reference HPLC-UV analytical technique. A good agreement was observed in the case of the off-line procedure, when both DPV and HPLC-UV measurements were carried out on samples withdrawn from the irradiation set-up. However, there is the notable exception of the triplet-state precursor AQ2S that yielded transformation intermediates interfering with the quantification of APAP by DPV. The same DPV electrochemical sensor, when immersed into the irradiated solution, was able to monitor in real-time the APAP photodegradation.

The second-order rate constant for the reaction between APAP and $HO^{\bullet}$ was assessed by using both the off-line and the real-time protocol. While the results obtained with off-line DPV- and HPLC-based measurements showed good agreement, a higher rate constant value was found with the real-time set-up. The difference with the off-line results is likely to be attributed to temperature variations of the irradiated solutions that, despite the adoption of some technical precautions, affected the electrochemical measurements.

Finally, although time-resolved techniques such as laser flash photolysis and pulse radiolysis are commonly used and reliable (but costly) methods to measure second-order rate constants, similar results could be achieved carrying out steady-state irradiation experiments with electrochemical monitoring of APAP photodegradation. To enable the development of an operational real-time DPV procedure for the determination of the reaction rate constants, we expect that at least the following implementations should be taken into account in future studies: (i) thermostatic conditions for the irradiated solutions; (ii) choice of chemically inert supporting electrolytes for the DPV measurements, and (iii) the use of photosensitizers that (unlike AQ2S) are not electroactive and that do not interact with the electrode surface.

Acknowledgments

MM and SB acknowledge financial support from Fondazione CRT, Torino, Italy (Project “Sviluppo ed applicazione di sensori elettrochimici per la determinazione di residui farmaceutici nelle acque”). The same project also provided financial support for the scholarship of LC.

References

Andreozzi, R., Caprio, V., Marotta, R., Vogna, D., 2003. Paracetamol oxidation from aqueous solutions by means of ozonation and H2O2/UV system. Water Res 37, 5, 993-1004. DOI:10.1016/S0043-1354(02)00460-8.

Avetta, P., Fabbri, D., Minella, M., Brigante, M., Maurino, V., Minero, C., Pazzi, M., Vione, V., 2016. Assessing the phototransformation of diclofenac, clofibric acid and naproxen in surface waters: Model predictions and comparison with field data. Water Res 105, 383-394. DOI: 10.1016/j.watres.2016.08.058.

Bedini, A., De Laurentiis, E., Sur, B., Maurino, V., Minero, C., Brigante, M., Mailhot, G., Vione, D., 2012. Phototransformation of anthraquinone-2-sulphonate in aqueous solution. Photochem Photobiol Sci 11, 1445. DOI: 10.1039/c2pp25111f.

Bisby, R.H., Tabassum, N., 1988. Properties of the radicals formed by one-electron oxidation of acetaminophen - a pulse radiolysis study. Biochem Pharmacol, 37, 2731-2738. DOI: 10.1016/0006-2952(88)90035-4.

Buxton, G. V., Greenstock, C. L., Helman, W. P., Ross, A. B., 1988. Critical review of rate constants for reactions of hydrated electrons, hydrogen atoms and hydroxyl radicals ($^{\bullet}OH/O^{-\bullet}$) in aqueous solution. J Phys Chem Ref Data 17, 513-886. DOI: 10.1063/1.555805.

Canonica, S., Hellrung, B., Mueller, P., Wirz, J., 2006. Aqueous Oxidation of Phenylurea Herbicides by Triplet Aromatic Ketones. Environ Sci Technol 40, 6636-6641. DOI: 10.1021/es0611238.

Carena, L., Minella, M., Barsotti, F., Brigante, M., Milan, M., Ferrero, A., Berto, S., Minero, C., Vione, D., 2017. Phototransformation of the herbicide propanil in paddy field water. Environ Sci Technol 51, 2695–2704. DOI: 10.1021/acs.est.6b05053.

Chiavazza, E., Berto, S., Giacomino, A., Malandrino, M., Barolo, C., Prenesti, E., Vione, D., Abollino O., 2016. Electrocatalysis in the oxidation of acetaminophen with an electrochemically activated glassy carbon electrode. Electrochim Acta 192, 139-147. DOI: 10.1016/j.electacta.2016.01.187.

Cory, R.M., McKnight, D.M., 2005. Fluorescence spectroscopy reveals ubiquitous presence of oxidized and reduced quinines in dissolved organic matter. Environ Sci Technol 39, 8142-8149. DOI**:** 10.1021/es0506962.

De Laurentiis, E., Prasse, C., Ternes, T. A., Minella, M., Maurino, V., Minero, C., Sarakha, M., Brigante, M., Vione D., 2014. Assessing the photochemical transformation pathways of acetaminophen relevant to surface waters: Transformation kinetics, intermediates, and modelling. Water Res 53, 235–248. DOI: 10.1016/j.watres.2014.01.016.

El Najjar, N. H., Touffet, A., Deborde, M., Journel, R., Vel Leitner, N. K., 2014. Kinetics of paracetamol oxidation by ozone and hydroxyl radicals, formation of transformation products and toxicity. Sep Purif Technol 136, 137-143, DOI: 10.1016/j.seppur.2014.09.004.

Erickson, P. R., Grandbois, M., Arnold, W. A., McNeill, K., 2012. Photochemical Formation of Brominated Dioxins and Other Products of Concern from Hydroxylated Polybrominated Diphenyl Ethers (OHPBDEs). Environ Sci Technol 46, 8174−8180. DOI: 10.1021/es3016183

Galbavy, E. S., Ram, K., Anastasio, C., 2010. 2-Nitrobenzaldehyde as a chemical actinometer for solution and ice photochemistry. J Photoch Photobio A 209, 186–192. DOI: 10.1016/j.jphotochem.2009.11.013.

Heberer, T., 2002. Occurrence, fate, and removal of pharmaceutical residues in the aquatic environment: a review of recent research data. Toxicol Lett 131, 5–17. DOI: 10.1016/S0378-4274(02)00041-3.

Hu, X., Yang, J., Yang, C., Zhang, J., 2010. UV/H2O2 degradation of 4-aminoantipyrine: A voltammetric study. Chem Eng J 161, 68–72. DOI: 10.1016/j.cej.2010.04.025.

Loeff, I., Treinin, A., Linschltz, H., 1983. Photochemistry of 9,10-Anthraquinone-2-sulfonate in Solution. 1. Intermediates and Mechanism. J Phys Chem 87, 2536-2544. DOI: 10.1021/j100237a017.

Mack, J., Bolton, J. R., 1999. Photochemistry of nitrite and nitrate in aqueous solution: a review. J Photoch Photobio A 128, 1–13. DOI: 10.1016/S1010-6030(99)00155-0.

Marchisio, A., Minella, M., Maurino, V., Minero, C., Vione, D., 2015. Photogeneration of reactive transient species upon irradiation of natural water samples: Formation quantum yields in different spectral intervals, and implications for the photochemistry of surface waters. Water Res 73, 145−156. DOI: 10.1016/j.watres.2015.01.016.

McNeill, K., Canonica, S., 2016. Triplet state dissolved organic matter in aquatic photochemistry: reaction mechanisms, substrate scope, and photophysical properties. Environ Sci-Proc Imp 18, 1381. DOI: 10.1039/c6em00408c.

Minella, M., Maurino, V., Minero, C., Vione, D., 2016. A model assessment of the ability of lake water in Terra Nova Bay, Antarctica, to induce the photochemical degradation of emerging contaminants. Chemosphere, 162, 91-98. DOI: 10.1016/j.chemosphere.2016.07.049.

OW/ORD Emerging Contaminants Workgroup, 2008. White Paper - Aquatic Life Criteria for Contaminants of Emerging Concern, Part I: General Challenges and Recommendations.

Peuravuori, J., 2012. Aquatic photochemistry of paracetamol in the presence of dissolved organic chromophoric material and nitrate. Environ Sci Pollut R 19, 2259-2270. DOI: 10.1007/s11356-011-0730-y.

Pojana, G., Fantinati, A., Marcomini, A., 2009. Occurrence of environmentally relevant pharmaceuticals in Italian drinking water treatment plants. Int J Environ An Ch 91, 537–552. DOI: 10.1080/03067310903531504.

Rahemi, V., Garrido, J. M. P. J., Borges, F., Brett, C. M. A., Garrido, E. M. P. J., 2015. Electrochemical sensor for simultaneous determination of herbicide MCPA and its metabolite 4-chloro-2-methylphenol. Application to photodegradation environmental monitoring. Environ Sci Pollut R 22, 4491–4499. DOI: 10.1007/s11356-014-3693-y.

Rapecki, T., Nowicka, A. M., Donten, M., Scholz, F., Stojek, Z., 2010. Activity changes of glassy carbon electrodes caused by their exposure to $OH^{\bullet}$ radicals. Electrochem Commun 12, 1531–1534. DOI: 10.1016/j.elecom.2010.08.026.

Stamatis, N. K., Konstantinou, I. K., 2013. Occurrence and removal of emerging pharmaceutical, personal care compounds and caffeine tracer in municipal sewage treatment plant in Western Greece. J Environ Sci Heal B 48, 800-813. DOI: 10.1080/03601234.2013.781359.

Stumpf, M., Ternes, T. A., Wilken, R-D., Rodrigues, S.V., Baumann, W., 1999. Polar drug residues in sewage and natural waters in the state of Rio de Janeiro, Brazil. Sci Total Environ 225, 135–141. DOI: 10.1016/S0048-9697(98)00339-8.

Szabó, L., Tóth, T., Homlok, R., Takács, E., Wojnárovits, L., 2012. Radiolysis of paracetamol in dilute aqueous solution. Radiat Phys Chem 81, 1503–1507. DOI: 10.1016/j.radphyschem.2011.11.036.

Ternes, T. A., 1998. Occurrence of drugs in German sewage treatment plants and rivers. Water Res 32, 3245–3260. DOI: 10.1016/S0043-1354(98)00099-2.

Vione, D., Minella, M., Maurino, V., Minero, C., 2014. Indirect photochemistry in sunlit surface waters: Photoinduced production of reactive transient species. Chem. Eur. J. 20, 10590–10606. DOI: 10.1002/chem.201400413.

Vogna, D., Marotta, R., Andreozzi, R., Napolitano, A., d'Ischia, M., 2004. Kinetic and chemical assessment of the UV/H2O2 treatment of antiepileptic drug carbamazepine. Chemosphere 54, 497–505. DOI: 10.1016/S0045-6535(03)00757-4.

Wei, L., Borowiec, J., Zhu, L., Zhang, J., 2012. Electrochemical investigation on the interaction of diclofenac with DNA and its application to the construction of a graphene-based biosensor. J Solid State Electr 16, 3817-3823. DOI: 10.1007/s10008-012-1815-3.

Yang, L., Y u, L. E., Ray, M. B., 2009. Photocatalytic Oxidation of Paracetamol: Dominant Reactants, Intermediates, and Reaction Mechanisms. Environ Sci Technol 43, 460–465. DOI: 10.1021/es8020099.

Zuccato, E., 2004. Prediction of the environmental load of pharmaceuticals contaminating the marine environment. A case for the Adriatic Sea. CIESM Workshop Monographs n° 26 CIESM, Monaco, pp. 51–54.

Zuccato, E., Castiglioni, S., Fanelli, R., 2005. Identification of the pharmaceuticals for human use contaminating the Italian aquatic environment. J Hazard Mater 122, 205–209. DOI: 10.1016/j.jhazmat.2005.03.001.

Zuccato, E., Castiglioni, S., Fanelli, R., Reitano, G., Bagnati, R., Chiabrando, C., Pomati, F., Rossetti, C., Calamari, D., 2006. Pharmaceuticals in the Environment in Italy: Causes, Occurrence, Effects and Control. Environ Sci Pollut R 13, 15 – 21. DOI: 10.1065/espr2006.01.004.